Optical Simulation of Black Silicon Surfaces using Geometric Randomisation and Unit-cell Based Averaging

Jack J. Tyson*, Tasmiat Rahman, Stuart A. Boden

School of Electronics and Computer Science, University of Southampton, UK
*Corresponding author. Email address: [redacted]

15th Photovoltaic Science, Application and Technology Conference

April 12, 2019

Abstract

In this work, we present a method of simulating the reflectance spectra of black silicon surfaces using the finite element method. Outlined is the design and verification of a new set of algorithm-controlled geometries, rendering a vast array of different structural permutations, whilst measuring the spectral response of each individually. Our model is focussed on the variation of these geometries within the limits of certain ranged parameters for quantities such as nanowire height, radius, pitch, bend and bunching. Also explored is the variation of nanowire positioning within the simulation domain, leading to the more accurate depiction of non-uniform spacing between any given pair. Reflectance data was collated and averaged from all the random models to reliably determine the reflectance of an entire b-Si surface. The comparison between simulated results and their real equivalents offers the possibility of a simulation model versatile enough to predict the spectra of new and unorthodox designs.

I. Introduction

Texturing of the semiconductor surface is commonly used to provide antireflection and light trapping in silicon PV devices. With the advancement of black silicon (b-Si) solar cell technologies presenting an increasing number of novel nanostructure designs, the need to model the optical performance characteristics of each is paramount. Already in-place are a vast array of time-proven options for the spectral modelling of silicon for photovoltaics. In more recent years, observations regarding how surface texturing enhances the performance of photovoltaic devices have become increasingly commonplace, with smaller and more intricate textures being developed.

The Transfer Matrix Method (TMM) is the go-to choice for modelling thin-film devices due to its robust simplicity, speed and accuracy [1]. It calculates how much incident light is reflected and transmitted at each interface between any two coupled domains [2]. TMM only looks at a model in one dimension, and thus is not capable of simulating any device without a planar surface morphology. Alternatively, traditional microscale surface texturing such as pyramids and isotextures, whereby the features are much larger than the wavelength of incident light, can be modelled by optical ray tracing (ORT) methods. However, ORT does not work with more modern nanoscale b-Si textures now being adopted by solar cell manufacturers, where surface features are often far smaller in size than the wavelength of incident light [3].

Alternatively, for these more complex morphologies, there lies the Fourier modal method (FMM) [4] and the finite-difference time domain (FDTD) method. Often, FDTD is the method of choice when simulating the materials for photovoltaic (PV) devices where it has also seen some success in the modelling of basic and relatively uniform nanotextures [5]. However, FDTD does not provide access to the intricacies of the simulation geometry available using the finite element method (FEM) [6]. Justification for the use of FEM over the benefits offered by FDTD comes down to this unparalleled level of geometric manipulation.

It has been demonstrated that b-Si is difficult to simulate accurately due to the more obscure surface morphologies presented in practice; that the surface of b-Si is inherently heterogeneous. For example, metal

assisted chemical etching (MACE) techniques produce randomly-distributed arrays of nominally vertical nanowires (NW) that often bend and clump together in bunches (see figure 1, left). All methods of device modelling can be said to rely wholly or in-part on some degree of periodicity, short of recreating and simulating an entire surface. To solve this problem, we have combined the geometry control of FEM alongside a set of mathematical algorithms designed specifically to randomise and simulate many unit-cells, each containing different NW patterns, whilst measuring the reflectance of each individually. An average can then be taken yielding, in theory, an accurate reflectance representative of an entire b-Si device.

II. Designing the Model Geometry

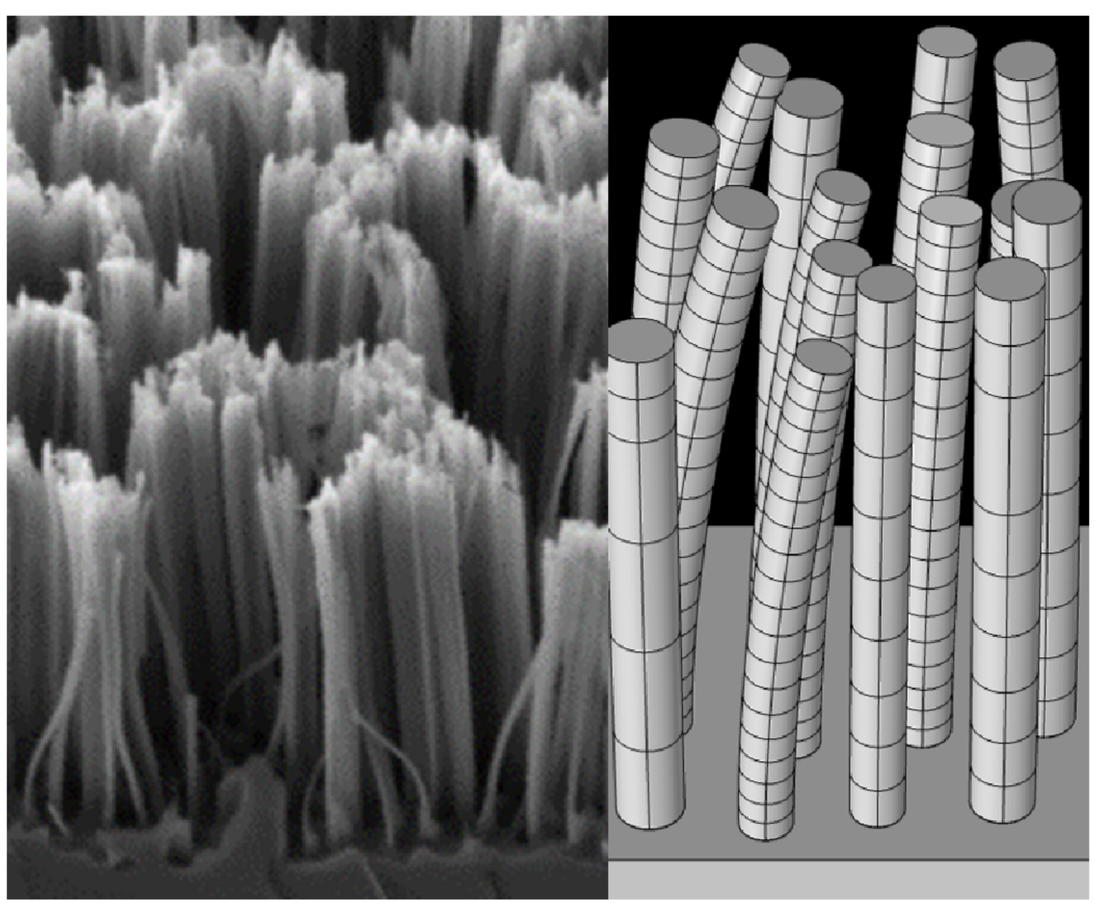

Figure 1: A scanning electron microscopy image of a black silicon surface etched by MACE into monocrystalline silicon (left), alongside our 4×4 nanowire geometry (right).

The simulation model used here was designed on COMSOL Multiphysics® v5.4†, and then computed using the IRIDIS 5 supercomputer providing multi-parallel task execution on up to 32 compute nodes simultaneously. The core of the simulation geometry is formed of four key components; two material domains and two perfectly matched layers (PMLs). The material domains were the silicon substrate and the air above it, whilst the PMLs were used to extend those domains infinitely away from the interface between them. An n-by-n square grid of silicon NWs could then be created at this interface, extruding outward from the silicon into the air. The air domain was elongated automatically to ensure complete encapsulation of all the NWs within the grid.

As previously stated, b-Si surfaces are not uniform in nature, and as a result statistically no two NWs can be exactly the same. In fact, the NWs forming a b-Si surface can have varying diameters, heights and orientations, whilst not necessarily forming equally spaced apart. They also often form with distinct bends. This is shown through the scanning electron microscopy (SEM) image in figure 1. To ensure each generated NW was different from the next, a series of interlinked pseudorandom functions and logical switches were employed alongside a single, variable input seed. Static parameters were created and used to provide a central value from which the pseudorandomised parameters would sit around. For example, the static NW height could be pre-set at 1 μm, causing their actual randomised heights to fall around this value within a given range. Pseudorandomised parameters for each individual NW held the following mathematical form:

$$r(S) = P + f_r(S) \tag{1}$$

Where r is the pseudorandomised parameter, P is the static parameter, f_r is the pseudorandom function, and S is an input seed in integer form. Each pseudorandom function used a uniform distribution with a mean of zero, yielding more realistic and controllable geometries. The range of the distribution was dependent on the parameter being randomised; different parameters, such as the radius or pitch, would not be varied within the same range as one another. Table 1 shows the variations applied by f_r for each given static parameter P. NW bending was achieved using a Bézier polygon employing a quadratic form-factor acting as a spine. A cylinder could then be extruded from the silicon substrate using the spine as a guideline, not only providing height but also curvature. All NWs were cylindrical with flat tops.

Static, P	**Randomised,** r
Height	$P \pm 0.075P$
Radius	$P \pm 0.30P$
Pitch	$P \pm 0.15P$
Bunching zone width	$P \pm 0.15P$

Table 1: Magnitude of applied variation onto each static parameter P by its pseudorandom function f_r.

Bunching is a trait often associated with much longer nanowires [7]. In the event that the height parameter was sufficiently large enough to require the inclusion of this trait for accuracy, the top of each spine needed to be influenced towards a 'bunching zone' for simulation domains inclusive of more than one

NW. 'Bunching zones' are virtual and have no substance within the model but are used to influence the x and y coordinates at the top of each spine, causing them to collectively gather within it. Only NWs that fall close enough to one of these zones, as defined by the 'bunching zone width', will be bunched. This is shown graphically in figure 2.

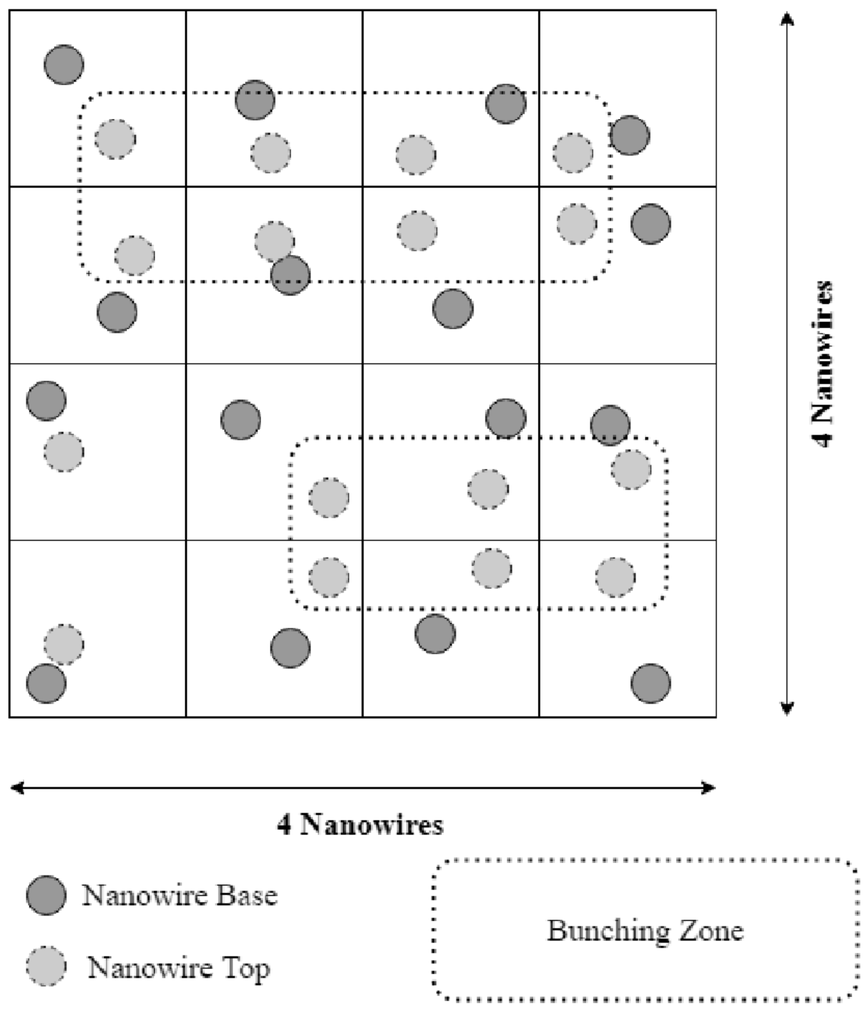

Figure 2: Bunching within a 4×4 unit-cell of nanowires.

III. Methodology

Convergence simulations were run to determine the largest possible size for the smallest mesh elements yielding consistent results for a reduced run-time. This value was then set for all simulation models where an averaging analysis, followed by a spectral sweep were performed. Wave optics based computational mathematics were used to generate electromagnetic (EM) stimuli and measure the total reflectance of each unit-cell. This was achieved through the application of a power transmission port at the interface between the silicon substrate and its PML. The power being transmitted through the substrate P_T was being measured and converted into a reflectance measurement using equation (2).

$$R_i(\lambda, S) = \frac{1 - P_T(\lambda, S)}{P_{\text{in}}(\lambda)} \tag{2}$$

All wavelength sweeps were run in the range 400:25:1000 nm, with an average taken at the number of sweeps required for convergence. Parameter variations were adjusted and their overall effect on the averaged reflectance was then determined. The reflectance of the real sample was completed in previous work [8] using a centre-mount integrating sphere setup employing a USB2000+ spectrometer from OceanOptics. A bare silicon sample was used as a reference for this measurement.

Results and Discussion

As shown in figure 3, it was found that convergence from running multiple full-wavelength sweeps occurred after taking a minimum of 10 averages. Given the computational resources and time required to execute a single sweep, the minimum number of sweeps possible were run rather than extending the overall runtime unnecessarily for no increase in average reflectance resolution.

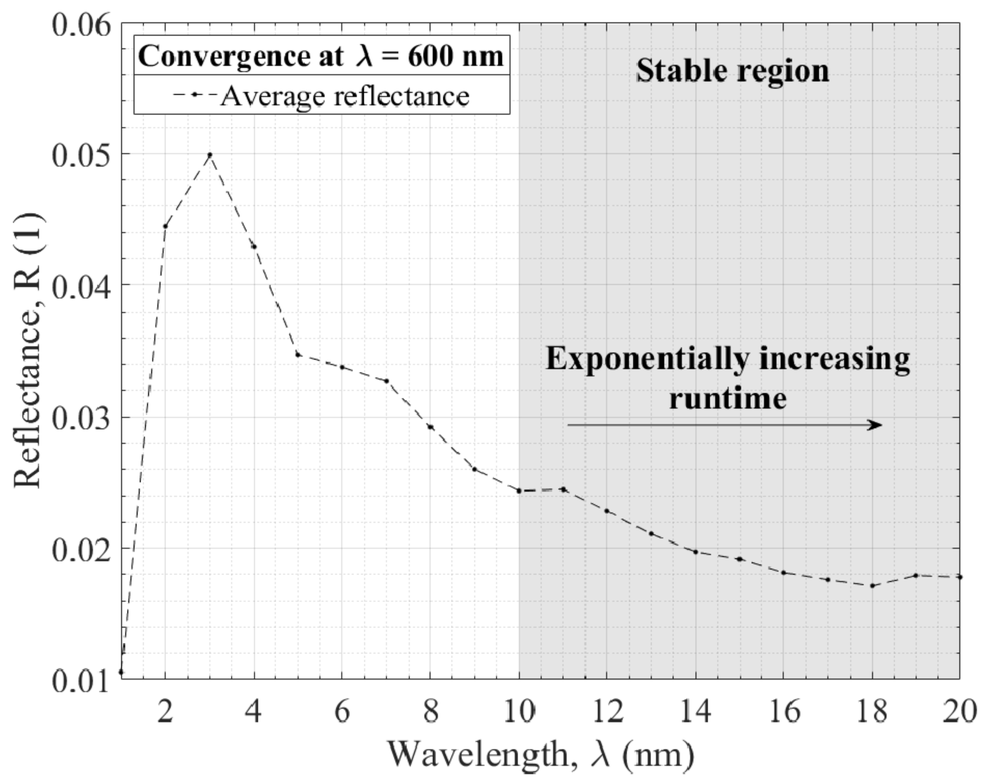

Figure 3: Demonstrating 4×4 unit-cell convergence.

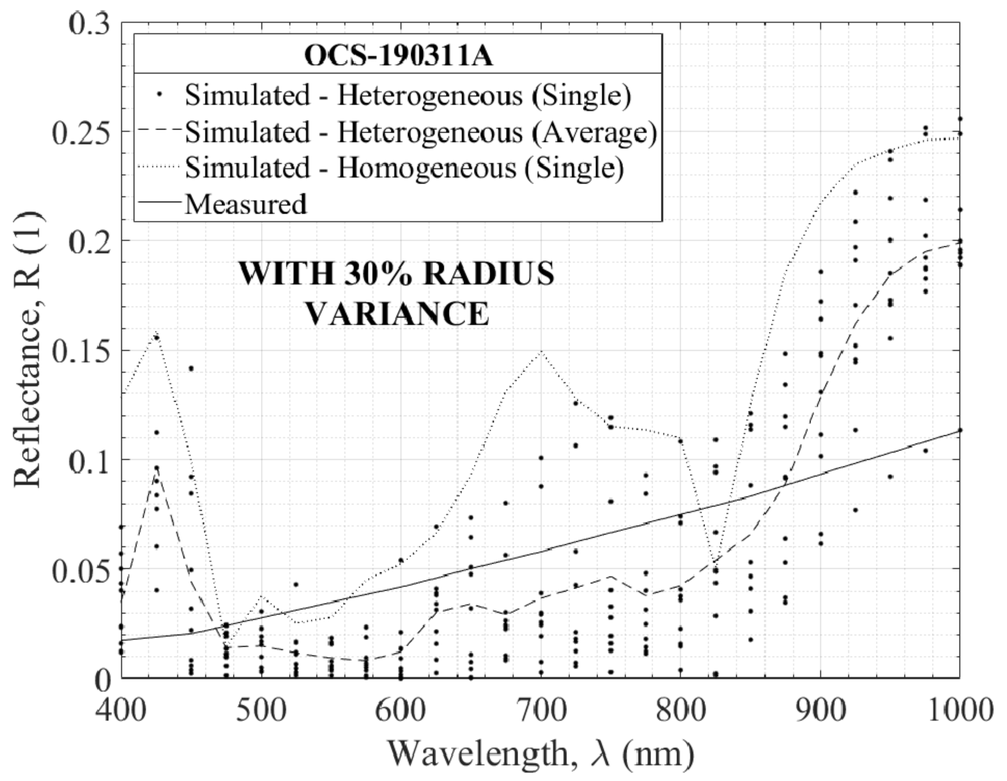

Figure 4: Reflectance of nanowire models with heterogeneity and homogeneity, and the real response.

The data shown in figure 4 shows the measured reflectance as having an average of 6% across the broadband spectrum, the heterogeneous simulations have an average of 6.5%, and the homogeneous had one of 12.2%. These metrics alone demonstrate the effectiveness of the averaging technique explored here,

as well as the effect of applying pseudorandomness to the simulation model. It can also be seen that the broadband reflectance for single model simulations were highly spread, with a range in the region of 10-15%. Furthermore, between wavelengths of 500 and 880 nm, the average reflectance representative of 10 different single models bound by the parameters outline in table 1 was within a 3.5% reflectance of the measured equivalent for 30% radius variance. This represented a moderately successful match for such a complex and stochastic model geometry, however it was important to theorise as to the difference observed here.

On the SEM analysis of real NWs, previous work has shown their structures, that is to say their footprints, are inconsistent with that used in the geometries here. Wholly cylindrical NWs are an optimistic and aliased definition, given that data showing real structures as having far different form-factors has been presented prior to this research [9, 10]. Simulation inaccuracies could have also been the result of insufficient grid size; our 4×4 NW geometry could theoretically be out-simulated by a 5×5 version or larger. Simulations of this size were undesirable and avoided due to how increasingly computationally expensive they become.

$$R_t(\lambda) \cong \bar{R}_m(\lambda, S) = \frac{1}{m}\left(\sum_{i=1}^{m}\left(R_i(\lambda, S)\right)\right) \qquad (3)$$

Despite our averaging approach to combat the need to increase this size, an essence of homogeneity becomes readily noticeable as essentially some m number of 4×4 grids simulated are repeated an infinite number of times to create a virtual full-scale device. As represented in equation (3), it can be shown that $\bar{R}_m(\lambda, S) \equiv R_t(\lambda)$ as $m \to \infty$, where $\bar{R}_m$ is the average reflectance of m NW grids and $R_t(\lambda)$ is the reflectance of an entire b-Si surface made-up of periods of these grids. Naturally, it is not possible to simulate an infinite number of grids, but accuracy of our average reflectance could have potentially been improved by increasing m beyond 10, though our investigations show the model as having already reached convergence at this point.

Conclusions

Our simulation model offers a previously unseen level of heterogeneity and control in contrast to other methods such as FDTD. Links were formed between model size, accuracy and convergence, as well as NW parameter variance and reflectance. Going forward, it is important to confirm the sources of inaccuracies within the presented model, and increase the level of heterogeneity further by inducing pseudorandom generation of the NWs shapes, possibly also extending the study to modify the currently flat-topped versions to having the rounded or pointed textures not uncommon to the real thing.

References

[1] H. J. El-Khozondar, M. M. Shabat, and A. N. AlShembari, "Characteristics of Si-solar cell (PV) waveguide structure using transfer matrix method," in *2017 International Conference on Promising Electronic Technologies (ICPET)*. IEEE, Oct. 2017.

[2] C. C. Katsidis and D. I. Siapkas, "General transfer-matrix method for optical multilayer systems with coherent, partially coherent, and incoherent interference," *Applied Optics*, vol. 41, no. 19, p. 3978, Jul. 2002.

[3] J. C. Pla, J. C. Duran, D. C. Skigin, and R. A. Depine, "Ray tracing vs. electromagnetic methods in the analysis of antireflective textured surfaces [of solar cells]," in *Conference Record of the Twenty Sixth IEEE Photovoltaic Specialists Conference - 1997*. IEEE, Oct. 1997.

[4] J. P. Hugonin, P. Lalanne, I. D. Villar, and I. R. Matias, "Fourier modal methods for modeling optical dielectric waveguides," *Optical and Quantum Electronics*, vol. 37, no. 1-3, pp. 107–119, Jan. 2005.

[5] D. Wu, X. Tang, K. Wang, and X. Li, "An analytic approach for optimal geometrical design of GaAs nanowires for maximal light harvesting in photovoltaic cells," *Scientific Reports*, vol. 7, no. 1, Apr. 2017.

[6] F. L. Teixeira, "Time-domain finite-difference and finite-element methods for maxwell equations in complex media," *IEEE Transactions on Antennas and Propagation*, vol. 56, no. 8, pp. 2150–2166, Aug. 2008.

[7] S. K. Srivastava, D. Kumar, P. K. Singh, M. Kar, V. Kumar, and M. Husain, "Excellent antireflection properties of vertical silicon nanowire arrays," *Solar Energy Materials and Solar Cells*, vol. 94, no. 9, pp. 1506–1511, Sep. 2010.

[8] T. Rahman and S. A. Boden, "Optical modeling of black silicon for solar cells using effective index techniques," *IEEE Journal of Photovoltaics*, vol. 7, no. 6, pp. 1556–1562, Nov. 2017.

[9] D. Kumar, S. K. Srivastava, P. K. Singh, M. Husain, and V. Kumar, "Fabrication of silicon nanowire arrays based solar cell with improved performance," *Solar Energy Materials and Solar Cells*, vol. 95, no. 1, pp. 215–218, Jan. 2011.

[10] J. Oh, H.-C. Yuan, and H. M. Branz, "An 18.2%-efficient black-silicon solar cell achieved through control of carrier recombination in nanostructures," *Nature Nanotechnology*, vol. 7, no. 11, pp. 743–748, Sep. 2012.

† *COMSOL Multiphysics is a registered trademark of COMSOL AB.*

This work has been supported by the Centre for Doctoral Training in New and Sustainable Photovoltaics (CDT-PV). The author of this work also acknowledges the use of the IRIDIS compute cluster, and associated support services at the University of Southampton, in the completion of this work.